TWO-FLUID COLLISIONAL MAGNETOHYDRODYNAMIC MODELING

BY

QUSAI AL SHIDI
B.S., UNIVERSITY OF TOLEDO (2008)

SUBMITTED IN PARTIAL FULFILLMENT OF THE REQUIREMENTS
FOR THE DEGREE OF DOCTOR OF PHILOSOPHY
DEPARTMENT OF PHYSICS AND APPLIED PHYSICS
UNIVERSITY OF MASSACHUSETTS LOWELL

Author .....
May 1, 2019

Certified by .....
Ofer Cohen
Assistant Professor
Thesis Supervisor

Accepted by .....

Abstract

Since the discovery of space plasmas, the space science community have been deriving fluid models of plasmas to best suit their scenarios. The simplest case is the ideal magnetohydrodynamic (MHD) model which assumes a collisionless perfectly-conducting plasma. Multi-fluid collisional MHD gives each fluid its own set of MHD equations while using collisions to set frictional and resistive terms between them. An important case of this nature is the solar chromosphere. The high density and relatively cold plasma ensures collision times are shorter than magnetic time scales. Multi-fluid collisional MHD has many cases from the Earth's ionosphere to stellar atmosphere and having a good grasp of the physics is important in studying these plasmas.

An acknowledgments page is optional.

Contents

List of Figures

List of Tables

Chapter 1

Introduction

The word 'plasma' was first used by Langmuir [1928] to describe oscillations in a gaseous electron medium [Tonks, 1967]. It is a state of matter that is can be described as an ionized gas. It is the most common form of baryonic matter in the universe. We default to plasma descriptions of the medium between stars and planets. The sun is, for example, made mostly of ionized hot plasma. It is made of plasma and shoots out supersonic plasma called the solar wind. This plasma does not entirely contact the Earth due to shielding resulting from the Earth's magnetic field. Due to plasma's ionization, it has a tendency to travel on magnetic field lines. This does not mean the Earth is completely shielded from the solar wind. Many space weather events are due to solar plasma's effect on the Earth and its magnetic field. The sun is a very active star that has spontaneous flares, coronal mass ejections (CME) and active regions. Thus spontaneous storms occur on Earth and our understanding of the sun and space plasmas is essential to protect ourself against storms.

In this dissertation, an attempt will be made to show the benefits and utility of multi-fluid magnetohydrodynamic (MHD) models. We will show that the solar chromosphere is a good case for this. The implementation will also be studied with careful use of good, modern computer science practices.

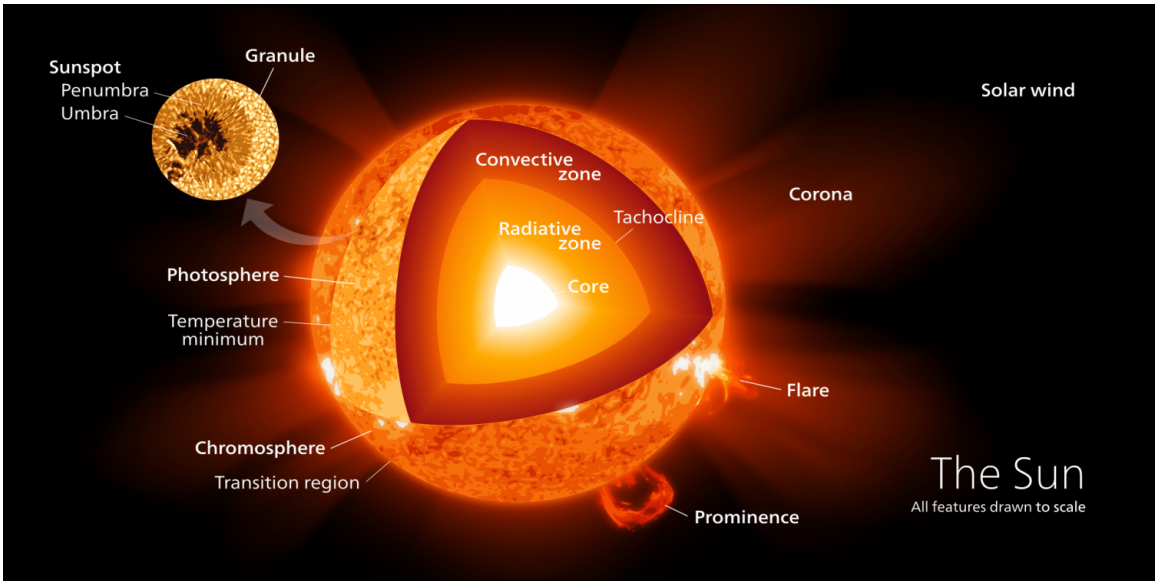

Figure 1-1: A more complicated view of the sun's structure and layers. [Image from `https://phys.org/news/2015-12-sun-energy.html`]

1.1 The Sun

Whenever we say 'the sun' we do not mean any star—we mean *our* star. The sun is a 4.6 billion year old yellow dwarf. It generates a lot of the energy we use for life on Earth. It creates this energy through nuclear fusion in its core, turning hydrogen into helium. The sun is mostly hydrogen with a small amount of helium and even smaller amounts of metal ions which require tremendous energy to fuse. The sun has six regions (from innermost to outermost): the core, the radiative zone, the covection zone, the photosphere, the chromosphere and the corona. The core is where the fusion happens. Here is where hydrogen is made into helium and other metals. The radiative zone and convection zone is where the energy travels radially upwards to wards the surface, the photosphere. The photosphere is the surface of the Sun. Here photons are trapped but the ones that do escape mimic black-body radiation (not perfectly). It is optically thick and is the white light we see when looking at the Sun. Above the photosphere is the atmospheric layer, the chromosphere, which we will go in much detail about in this dissertation. Above that, is the corona which is what gives the sun its tendrils and the hair we give our cartoon drawings of the sun.

1.1.1 The Chromosphere

The chromosphere is the interface between the surface, the photosphere, and the outer atmosphere, the corona. The plasma in it is partially ionized which means it consists of two kinds of plasma: ionized (charged) plasma, and neutral (uncharged) plasma. This means the charged plasma is affected by Lorentz forces while the uncharged plasma is not. This is a result of the temperature of the chromosphere and the composition of the plasma convected in the convection zone. The plasma has a high temperature in Earth standards but to the sun it is relatively cold. The temperature of the corona, which keep in mind is the outermost layer, is in the million of degrees in Kelvin. While most of the chromosphere and the photosphere is 5000K-6500K. This discrepancy in the temperature of the lower layers to the higher layers is called the coronal heating problem. The coronal heating problem is an outstanding problem in physics which makes understanding the chromosphere of special importance. Why is the corona hotter than the chromosphere?

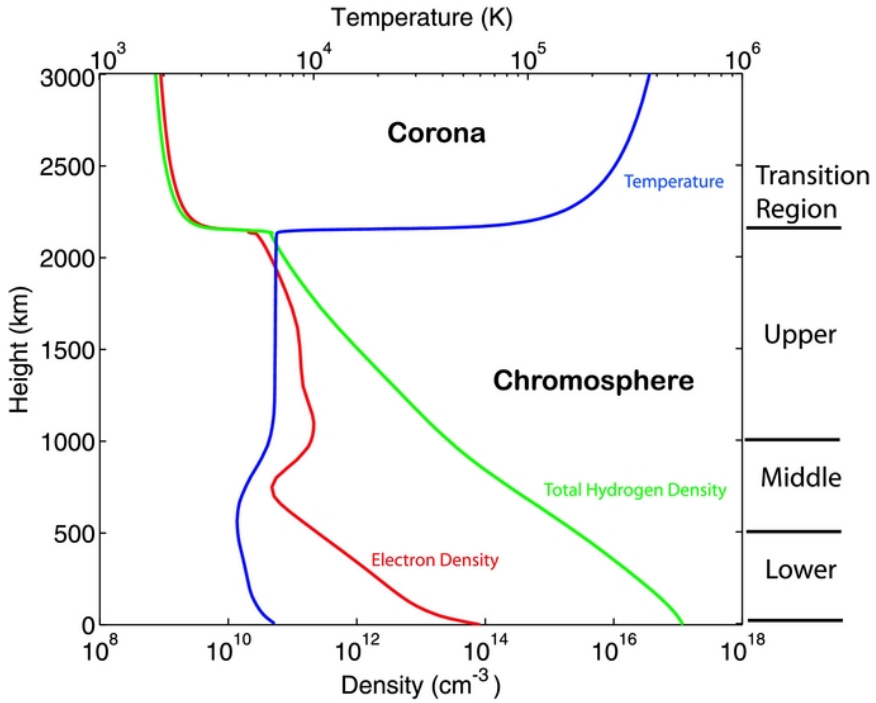

Figure 1-2: A view of the upper, middle and lower chromosphere. The chromosphere is partially ionized and is much colder than the corona (above the transition region). [Song and Vasyliūnas, 2014, Avrett and Loeser, 2008]

1.2 Space Weather

The term space weather refers to weather effects found above our immediate atmosphere which is conversely named terrestrial weather. It focuses on the conditions and changes found between the Sun, the Earth and even behind the Earth along its night time. The Earth's surface magnetic field strength is in the 0.5G range [Finlay et al., 2010] and that is strong enough to shield most of the solar wind headed our direction. However, magnetic reconnection events between the Earth's magnetosphere (the sphere of Earth's magnetic influence) and the interstellar medium allows solar wind particles to enter the Earth's atmosphere. This can manifest itself in harmless weather, like auroras, or more harmful weather, like geomagnetic storms.

1.2.1 Motivation: A storm is coming

In 1859, a famous (or infamous) geomagnetic storm hit the Earth. Fortunately, we did not sprawl global electrical power grids at the time or it would have had devastating effects. It was caused by a CME observed by Richard C. Carrington and was thusly named the Carrington Event. Depending on the strength of the geomagnetic storm (which happens frequently at higher/lower latitudes due to night side reconnection) it may reach mid-latitude areas which we habitate. Here geomagnetic storms due to the quick changes in magnetic fields and the law of induction cause ground induced currents (GIC) that can have damaging effects to any ground based electrical devices.

The Carrington event was our last encounter with a storm of that scale, that does not mean we have not had any near misses. In 2012, a coronal mass ejection that has the strength and size comparable to the previously mentioned Carrington event almost hit the Earth. It missed the Earth by nine days [Baker et al.]. Unlike in 1859, the world of 2012 was filled with electrical power grids. The internet is part of our daily lives and still relies on ground based electrical wiring.

1.2.2 Where does the chromosphere fit into this?

Chapter 2

Collisional Plasmas

Although plasmas are classically defined as charged gasses, they can coexist with neutral plasma based on the temperature and pressure conditions surrounding them. This means we have two gas mediums, one with the ability to feel Lorentz forces and another that acts like a non-charged fluid. This will generate friction between the fluids when they are moving at different velocities. Due to collision rates being proportional to fluid density and temperature, there can exist a limit in which collision rates are larger than ionization/recombination rates of ions and therefore the fluid becomes collisional. In the reverse case a single-fluid is an apt description as the existence of two-fluids matters largely on the chemistry rather than the collisions. We will be focusing on hydrogen plasmas for our chromosphere case in Chapter 4 and in that case two-fluids will be investigated.

2.1 Magnetohydrodynamics

Magnetohydrodynamics (MHD) is a fluid approximation of plasma popular amongst macroscopic studies of space plasmas. In order to arrive at the fluid approximation we must first look at the particles first and ensure the approximation is appropriate for our case. All of physics is a model and to go from the kinetic theory of plasmas by modelling particles to MHD plasmas by modelling fluids there must be a derivation since there are less assumptions in the kinetic theory than there are in MHD.

2.1.1 Kinetic Theory

We start by assuming an ensemble phase space of particles $f(\mathbf{x}, \mathbf{v}, t)$ called the distribution function. $\mathbf{x}$ is the location of the particle distribution in space, $\mathbf{v}$ is the velocity distribution and t is the time. To study the distribution function's evolution through time we take the full derivative with respect to time $\frac{df}{dt}$ which by the product rule turns out to be:

$$\frac{\partial f}{\partial t} + \frac{\partial \mathbf{x}}{\partial t} \cdot \nabla_{\mathbf{x}} f + \frac{\partial \mathbf{v}}{\partial t} \cdot \nabla_{\mathbf{v}} f = (\frac{\delta f}{\delta t})_{collisions} \tag{2.1}$$

This is called the Boltzmann equation. The term on the right hand side exists due to collisions changed the distribution function in its own way, this also include collisional ionization and other collisional effects that would change the distribution of particles. Simplifying the equation further by substituting how we expect the bulk particles to interact with fields we can get:

$$\frac{\partial f}{\partial t} + \mathbf{v} \cdot \nabla_{\mathbf{x}} f + \frac{q}{m}(\mathbf{E} + \mathbf{v} \times \mathbf{B}) \cdot \nabla_{\mathbf{v}} f = (\frac{\delta f}{\delta t})_{collisions} \tag{2.2}$$

Where q is the charge of the particle, m is the mass of the particle, $\mathbf{E}$ is the electric field and $\mathbf{B}$ is the magnetic field.

This is the kinetic theory of plasmas. The assumptions made here are probability distributions of particles instead of singular particle effects. There are simulations and codes that model particles directly but because of the large memory size of such simulations the region of study must be very small.

2.1.2 Moments of the Distribution

In order to arrive at the macroscopic variables we must make an assumption about the distribution of the fluid. This is the most fundamental assumption of MHD is that the distribution of the particles are behaving like a Maxwellian velocity distribution. If it is not the case that the velocity distribution is Maxwellian then the approach of MHD is challenged and must be rewritten and integrated differently. The Maxwellian

velocity distribution is common in space plasmas that are in thermal equilibrium with itself which lends to the popularity of MHD.

$$f(v) = n(\frac{m}{2\pi k_B T})^{3/2} \exp{(-\frac{mv^2}{2k_B T})} \tag{2.3}$$

Where $v = |\mathbf{v}|$ is the speed, k_B is the Boltzmann constant and T is temperature. This is assuming a Maxwellian velocity distribution over a thermal equilibrium and a thermal speed.

To arrive at the MHD equations we start to take the 'velocity moments' of the equations in order to have macroscopic variables that don't depend on phase speed.

$$Moment_a(\mathbf{x}, t) = \int \mathbf{v}^a f(\mathbf{x}, \mathbf{v}, t) d\mathbf{v} \tag{2.4}$$

Here a is the order of the moment. The first few moments are of interest. The zeroth moment is the continuity equation.

$$\frac{\partial n_s}{\partial t} + \nabla \cdot (n_s \mathbf{v}_s) = (\frac{\delta n_s}{\delta t})_{source} \tag{2.5}$$

Each species, s, of fluid has its own continuity equations but may be related by the source terms. The source terms come from integrating the collisional ionization, radiative recombination, etc.

The first order moment will give us the momentum equations:

$$\frac{\partial n_s \mathbf{v}_s}{\partial t} + \nabla \cdot (n_s \mathbf{v}_s \mathbf{v}_s + \frac{\mathbf{P}_s}{m_s}) - n_s \frac{q}{m_s}(\mathbf{E} + \mathbf{v}_s \times \mathbf{B}) = (\frac{\delta n_s \mathbf{v}_s}{\delta t})_{source} \tag{2.6}$$

Where $\mathbf{P}_s$ is the kinetic pressure tensor and can be simplified to the ideal gas law $P_s \mathbf{I} = n_s k_B T_s \mathbf{I}$ if applicable. The source terms due to the zeroth order also exists here as well as frictional terms that may appear in multifluid cases. It is apparent that this equation is fluid-like, a form of the Navier-Stokes equation and hence the naming of these equations as hydrodynamic.

To close the system equations we need one more for the pressure shown previously.

So integrating for the second moment gives:

$$\frac{\partial E_s}{\partial t} + \nabla \cdot (\mathbf{v}_s E_s) + \nabla \cdot \mathbf{q}_s = (\frac{\delta E_s}{\delta t})_{source} \tag{2.7}$$

Where q is the heat flow tensor which can be approached in multiple ways and E is the total energy:

$$E_s = e_s + \frac{1}{2} m_s {v^2}_s + E_{potential} \tag{2.8}$$

Here e is the internal energy and the potential energy is based on the momentum equation's extra acceleration terms like the fields or gravitational potential energy if included.

2.1.3 Multi-fluid MHD

In order to make our code capable to solve the equations shown in the previous section (Section 2.1.2) further approximations must be done. The three fluids of interest in a hydrogen plasma that includes neutrals are hydrogen ions, electrons and neutral hydrogen. Our plasma is collisional and in partially ionized plasmas we can use the Krook collision term.

$$(\frac{\delta f}{\delta t})_{collisions} = \nu_n (f_n - f) \tag{2.9}$$

Where subscript n is the neutral species and ν is the collision rate. We can find the collision rate simply by using the collision cross-section of neutral particles and the average thermal speed. The average thermal speed is used because temperature in the case of MHD is based on the 'peculiar' speeds of the particles (i.e. particles with velocity other than that of the bulk plasma). This way peculiar velocities contribute to collisions because if both fluids are moving in the same direction.

$$\nu_n = n_n \sigma_n < v > \tag{2.10}$$

The thermal speed is a function of temperature and under the Maxwellian ve-

locity distribution assumption, σ is the collisional cross-section which can be found in the literature through experiments. The collisional cross-section between ion and electrons include Coloumb effects as well.

The moment equations (Equation 2.5-2.7) for the three species will look like this:

$$\frac{\partial n_i}{\partial t} + \nabla \cdot (n_i \mathbf{v}_s) = S - L \tag{2.11}$$

$$\frac{\partial n_e}{\partial t} + \nabla \cdot (n_e \mathbf{v}_s) = S - L \tag{2.12}$$

$$\frac{\partial n_n}{\partial t} + \nabla \cdot (n_n \mathbf{v}_s) = L - S \tag{2.13}$$

$$\frac{\partial n_i \mathbf{v}_i}{\partial t} + \nabla \cdot (n_i \mathbf{v}_i \mathbf{v}_i + \frac{\mathbf{P}_i}{m_i}) - n_i \frac{q_i}{m_i} (\mathbf{E} + \mathbf{v}_i \times \mathbf{B}) = -\sum_{i \neq s} [n_i \nu_{is} (\mathbf{v}_i - \mathbf{v}_s)] + \frac{1}{m_i} (S m_n \mathbf{v}_n - S m_e \mathbf{v}_e - L m_i \mathbf{v}_i) \tag{2.14}$$

$$\frac{\partial n_e \mathbf{v}_e}{\partial t} + \nabla \cdot (n_e \mathbf{v}_e \mathbf{v}_e + \frac{\mathbf{P}_e}{m_e}) - n_e \frac{q_e}{m_e} (\mathbf{E} + \mathbf{v}_e \times \mathbf{B}) = -\sum_{e \neq s} [n_e \nu_{es} (\mathbf{v}_e - \mathbf{v}_s)] + \frac{1}{m_e} (S m_n \mathbf{v}_n - S m_i \mathbf{v}_i - L m_e \mathbf{v}_e) \tag{2.15}$$

$$\frac{\partial n_n \mathbf{v}_n}{\partial t} + \nabla \cdot (n_n \mathbf{v}_n \mathbf{v}_n + \frac{\mathbf{P}_n}{m_n}) = -\sum_{n \neq s} [n_n \nu_{es} (\mathbf{v}_n - \mathbf{v}_s)] + \frac{1}{m_n} (L(m_i \mathbf{v}_i + m_e \mathbf{v}_e) - S m_n \mathbf{v}_n) \tag{2.16}$$

S and L are source and loss terms respectively due to chemistry processes like ionization and recombination. These are three-fluid MHD equations if the only ion considered is the hydrogen ion.

2.1.4 Two-fluid MHD

The ion and electron fluid can be simplified further to be one plasma that tracks the center of momentum between the two. Plasmas are typically quasi-neutral, it has as many positive charges as negative ones. Any imbalance in the charge will create a strong electric field within the plasma and strongly attract outside sources of charges until it is quasi-neutral again. In single hydrogen ion case that means:

$$n_i = n_e \tag{2.17}$$

This can simplify the current density equation as well:

$$\mathbf{J} = n_i \mathbf{v}_i - n_e \mathbf{v}_e = n_i(\mathbf{v}_i - \mathbf{v}_e) \tag{2.18}$$

To simplify the three MHD equations (Equations 2.14-2.16) we can take the multiple of their masses and add Equation 2.14 and 2.15.

$$\begin{aligned} &\frac{\partial \rho_i \mathbf{v}_i + \rho_e \mathbf{v}_e}{\partial t} + \nabla \cdot (\rho_e \mathbf{v}_e \mathbf{v}_e + \rho_i \mathbf{v}_i \mathbf{v}_i + \mathbf{P}_i + \mathbf{P}_e) - \mathbf{J} \times \mathbf{B} \\ &= -\rho_i \nu_{in}(\mathbf{v}_i - \mathbf{v}_n) - \rho_e \nu_{en}(\mathbf{v}_e - \mathbf{v}_n) + (S m_n \mathbf{v}_n - L m_i \mathbf{v}_i - L m_e \mathbf{v}_e) \end{aligned} \tag{2.19}$$

The ρ here is the mass density of the fluid. Using the induction equation Maxwell's equations we can simplify $\mathbf{J} \times \mathbf{B}$ further.

$$\mathbf{J} \times \mathbf{B} = \frac{1}{\mu_0}(\nabla \times \mathbf{B}) \times \mathbf{B} = -\nabla \cdot (\frac{B^2}{2\mu_0}\mathbf{I} - \mathbf{B}\mathbf{B}) \tag{2.20}$$

This way we can have a magnetic flux and make use of our conservative scheme in Section 3.1.2. Finaly by dividing by $m_i + m_e$ to Equation 2.19 we can find the center of momentum velocity and simplify the equation one last time:

$$\mathbf{V} = \frac{\rho_i \mathbf{v}_i + \rho_e \mathbf{v}_e}{\rho_i + \rho_e} \tag{2.21}$$

$$\mathbf{v}_i = \mathbf{V} + \frac{\rho_e}{\rho_i + \rho_e}\frac{1}{ne}\mathbf{J} \sim \mathbf{V} + \frac{m_e}{m_i}\frac{\mathbf{J}}{ne} \tag{2.22}$$

$$\mathbf{v}_e = \mathbf{V} - \frac{\rho_i}{\rho_i + \rho_e}\frac{1}{ne}\mathbf{J} \sim \mathbf{V} - \frac{\mathbf{J}}{ne} \tag{2.23}$$

$$\begin{aligned} &\frac{\partial \rho \mathbf{V}}{\partial t} + \nabla \cdot (\mathbf{K} + \frac{B^2}{2\mu_0}\mathbf{I} - \mathbf{BB}) \\ &= -(\rho_i \nu_{in} + \rho_e \nu_{en})(\mathbf{V} + \frac{m_e}{m_i}\frac{\mathbf{J}}{ne} - \mathbf{v}_n) + \frac{m_e}{e}(\nu_{en} - \nu_{in})\mathbf{J} \\ &+ [Sm_n\mathbf{U} - Lm_i(\mathbf{V} + \frac{m_e}{m_i}\frac{\mathbf{J}}{ne}) - Lm_e(\mathbf{V} - \frac{\mathbf{J}}{ne})] \end{aligned} \tag{2.24}$$

The dynamic pressure and thermal pressures have been combined into one kinetic tensor term $\mathbf{K}$. The elementary charge is e. $\mathbf{U}$ is the neutral velocity.

2.2 Generalized Ohm's Law

Chapter 3

Implementation

Computational fluid dynamics is a well studied field in computer science, numerics and engineering. Many of its principles can be appled to MHD due to the fluid nature of its equations. We will be focusing on only the ones implementedd in the code my for this dissertation, the Collisional Multi-Fluid ion (CoMFi) code made for the chromosphere case which will be explored in more detail in the upcoming chapter (Chapter 4). The code is an ever-evolving code that uses Graphical Processing Units (GPUs) instead of the common CPUs you see for MHD codes. This is to implement MHD that makes use of the frontiers of computer technology. GPUs were made for graphical operations in video games. This means they are specifically designed to be very fast at matrix rotations, translations and other linear algebra. In this chapter we will explore proper general purpose GPU programming techniques for solving differential equations and the schemes used alongside it. CoMFi is written in C++ using ViennaCL for GPU linear algebra template programming and Armadillo for setting up the matrices on the CPU (the reason for this will be discussed in).

3.1 Schemes

CoMFi uses the conservative MHD equations therefore conservative schemes are of interest. This makes use of the conservative variables unknowns as opposed to the primitive variables (nv as opposed to v). This way we can use a finite-volume-method

and conserve these quantities to the machine rounding error. Conservative schemes are also known to do well at capturing shocks and the chromosphere is a region where we expect such shocks to exist.

$$\frac{\partial \mathbf{u}}{\partial t} + \nabla \cdot \mathbf{F}(\mathbf{u}) = 0 \tag{3.1}$$

The above equation is a general euler equation demonstrating a conservation law problem. The quantity to be conserved is $\mathbf{u}$ and is a function the flux $\mathbf{F}$. We will be considering the linear case for simplicity however MHD has demonstrably non-linear terms as the flux (e.g. Equation 2.14) but it can easily follow from this linear case. The point is to show the total volume is conserved:

$$\frac{d\mathbf{u}}{dt} + \frac{1}{V}\oint \mathbf{F} \cdot \mathbf{n} dS \tag{3.2}$$

In codes designed to solve differential equations numerically we must decide on the discretization. Since we are using a finite-volume-method we are discretizing the domain by cells with density quantities in them. The code is discretized in cells existing in cartesian coordinates (rectangular cells) so we are tasked to find the values of the variables at the cell faces in order to conserve the volume.

We would also like a total-variation-diminishing (TVD) scheme, this is because spatial derivatives are approximated on a computer. If we take a taylor series of a derivative from one cell to another and compare with an approximate derivative like $\frac{u(x+\Delta x)-u(x-\Delta x)}{2\Delta x}$ we see that there are many higher order terms missing. Taking the fourier analysis of these terms show that any high-frequency errors may compound (sometimes referred to as spurious oscillations). This can be fixed by schemes that ensure the total variation TV is diminishing.

$$\frac{dTV}{dt} = \frac{d}{dt}\int |\frac{\partial u}{\partial x} dx \leq 1 \tag{3.3}$$

Therefore, for the the purpose of our code, we will use the Total-Variation-Diminishing Monotonic Upwind Scheme for Conservation Laws (TVD-MUSCL).

3.1.1 Flux limiters

To conserve the cell's quantities we must be able to approximate the quantities on the cell edges. At the same time we must perserve monotonicity to avoid the oscillations. This can be achieved through flux limiters. The utility of the flux limiters is to turn the scheme into a first-order upwind scheme in sharp discontinuities and a high-resolution scheme when the solution is smooth.

$$u_{j+1/2} = u_j + \frac{1}{2}\phi(r_j)(u_{j+1} - u_j) \tag{3.4}$$

$$r_j = \frac{u_j - u_{j-1}}{u_{j+1} - u_j} \tag{3.5}$$

Subscript j is the discretized cell location with quantity u. The ratio of successive gradients r determines how strongly the flux limiter acts to find the extrapolated cell edge variable. The flux limiter ϕ includes the cells around edge more readily the smoother the solution is ($r > 0$), or sharp it is ($r < 0$) in which case the flux limiter is zero ($\phi = 0$). These are the properties flux limiters must abide in order to turn the scheme upwind in sharp gradients or high-resolution in smoother gradients. The above equation is a linear reconstruction of a cell edge. Other reconstructions exist but are more diffusive and avoids the shock-capturing goal of the code.

We have some freedom in choosing how to set the flux limiter. Many flux limiters have been made and studied in the past. The simplest flux-limiter is the minmod.

$$\phi_{minmod}(r) = \max(0, \min(1, r)), \lim_{r\to\infty} \phi(r) = 1 \tag{3.6}$$

The CoMFi code provides several flux limiters and finding the best one is a matter of trial and error. The limiter used by default is the van Albada limiter.

$$\phi_{va}(r) = \frac{r^2 + r}{r^2 + 1}, \lim_{r\to\infty} \phi(r) = 1 \tag{3.7}$$

Implementing these on a computer however is not a trivial task. Many initial conditions require the entirety of the domain be the same number for instance. In

that case we get an $r = \frac{0}{0}$ and this causes a computer to return NaN (not a number). Setting to $r = 0$ is approriate but requires extra coding. A work around is to add a small number ϵ to the denominator known as the machine epsilon to avoid these cases.

$$r_j = \frac{u_j - u_{j-1}}{u_{j+1} - u_j + \epsilon(u_{j+1} - u_j + 1)} \tag{3.8}$$

3.1.2 TVD-MUSCL

The TVD-MUSCL scheme reconstructs 'left' (L) and 'right' (R) states of the cell edge variables.

$$u^L_{j-1/2} = u_{j-1} + \frac{1}{2}\phi(r_{j-1})(u_j - u_{j-1}) \tag{3.9}$$

$$u^L_{j+1/2} = u_j + \frac{1}{2}\phi(r_j)(u_j - u_{j-1}) \tag{3.10}$$

$$u^R_{j-1/2} = u_j + \frac{1}{2}\phi(r_j)(u_{j+1} - u_j) \tag{3.11}$$

$$u^R_{j+1/2} = u_{j+1} + \frac{1}{2}\phi(r_{j+1})(u_{j+1} - u_j) \tag{3.12}$$

With the left and right extrapolated variables we may construct a flux.

$$F^*_{j-1/2} = \frac{1}{2}([F(u^R_{j-1/2}) + F(u^L_{j-1/2})] - \lambda_{j-1/2}[u^R_{j-1/2} - u^L_{j-1/2}]) \tag{3.13}$$

$$F^*_{j+1/2} = \frac{1}{2}([F(u^r_{j+1/2}) + F(u^l_{j+1/2})] - \lambda_{j+1/2}[u^r_{j+1/2} - u^l_{j+1/2}]) \tag{3.14}$$

Here $Fu = \lambda u$ are the eigenvalues of the variables. This in physical terms means the largest wave speeds of the system. Typically for the ion plasma it is the fast-mode speed and for the neutrals it is the sound speed. It's important to note in conservative MHD this is only the wave speed (c_{fast}) and not the same as the fastest

speed of information propagation ($v + c_{fast}$). The diffusive terms proportional to λ are meant to avoid the oscillations and if they are larger than they need to be the solution will be more diffusive.

3.2 Time Integration

3.3 Architecture

It is important in scientific computing not to reinvent the wheel. There are many libraries, particularly C++ libraries, that use template programming to make it easier to write linear algebra in code. It is always easier to add an entire vector with one + sign than looping through each element of the two vectors and adding each. For this reason we can avoid low-level programming like Fortran for CPUs or OpenCL and CUDA for GPUs because the Basic Linear Algebra Subroutines (BLAS) have already been written and abstracted by someone else. C++ is a language that is all about abstraction and speed. There is a pervasive myth that if you want to do scientific computing you must use Fortran or CUDA but this is not true and is usually reinforced by scientists' lack of understanding of computer science and/or bad code.

The code uses to template expression libraries in C++. Template expression is how C++ abstracts operators such as +, - and / to deal with one variable and the next and call the low level BLAS functions. The libraries used are Armadillo for CPU. This is a code typically used for Machine Learning applications so speed and big data is its focus. For GPU programming ViennaCL is used, it's a library used by PETSc for its GPU portion. However, at the time of this writing, PETSc's GPU code is not fully developed so ViennaCL is used directly. Luckily, ViennaCL interfaces with Armadillo well and there exists copy constructors to go from shared memory to GPU memory.

Matrices *must* be built on the CPU. Accessing GPU elements individually is a slow process that is limited by the PCI-e speed and when the machine code (running on cpu) is asked to go back and forth, we get slow code. Best practice is to first build

a matrix on the CPU then copy to the GPU.

3.3.1 Data Structure

When using the semi-implicit method a linear system $Ab^{n+1} = b$ must be solved. We must think of an approriate ordering of our vector in terms of the where the unknowns must be in the elements of the vector. For GPU programming in order to take advantage of its matrix operations speeds due to its many cores we must also be easily able to change back and forth between matrix and vector form between the implicit and explicit portions of the solution. A good ordering for a two-dimensional domain looks like this:

$$b = \begin{bmatrix} u_{0,00} \\ \vdots \\ u_{0,i0} \\ \vdots \\ u_{0,ij} \\ \vdots \\ u_{w,ij} \end{bmatrix} \tag{3.15}$$

The subscripts i and j describe the location of the cell in the x and y axis respec-

tively and w are the scalar unknowns.

$$u_w = \begin{bmatrix} B_x \\ B_\perp \\ B_z \\ n_i \\ n_n \\ n_i V_x \\ n_i V_\perp \\ n_i V_z \\ n_n U_x \\ n_n U_\perp \\ n_n U_z \\ T_i \\ T_n \\ \Phi \end{bmatrix} \tag{3.16}$$

This can be easily resized into a matrix of the form:

$$B = \begin{bmatrix} u_{0,00} & \cdots & u_{w,00} \\ \vdots & \ddots & \vdots \\ u_{0,i0} & \cdots & u_{w,i0} \\ \vdots & \ddots & \vdots \\ u_{0,ij} & \cdots & u_{w,ij} \end{bmatrix} \tag{3.17}$$

This has the benefits of making good use of GPU programming by using the parallelism found in matrix operations. This also means you can share boundary conditions by taking or providing rows for this matrix in chunks. You can do operations on specific unknowns by taking the approriate column.

3.4 Normalization

The unknowns in the simulations must be normalized. This is typical good practice in numerics when we're dealing with computers due to how computers deal with floating point number. Since computers deal with discrete numbers the floating point number line is discrete and also less regular than the real number line. There are more floating point numbers between -1 and 1 than there are between 10 and 11 for example. For this purpose, it is important to find a way in which the common numbers we will be dealing with be normalized to 1. We can do this by having, usually, the largest numbers found in the simulation domain be the normalizing constants.

3.4.1 Constants

The normalization constants were chosen for the chromospheric case we study in Chapter 4. For a more in-depth discussion on why these were chosen see Section 4.1.

Table 3.1: Normalization constants chosen for the chromospheric simulation

Magnetic Field	B_0	0.1 T
Length	L_0	2.1×10^6 m
Number Density	n_0	1.0×10^{20} m^{-3}
Mass	$m_0 = m_i$	$1.672621898 \times 10^{27}$ kg
Vacuum Permeability	μ_0	1.2566370614×10^6 Vs/A/m
Charge	e_0	$1.6021766208 \times 10^{19}$ C
Boltzmann Constant	k_B	$1.38065 \times 10^{-}23$ J/K
Velocity	$V_0 = \frac{B_0}{\sqrt{\mu_0 m_i n_0}}$	2.18×10^8 m/s
Pressure	$p_0 = \frac{{B_0}^2}{\mu_0}$	8.0×10^3 Pa
Temperature	$T_0 = \frac{p_0}{n_0 k_B}$	5.79438×10^6 K

3.4.2 Normalized Equations

Once we have our normalization constants we may normalize the equations. Replacing each term by its normalized version reduces the equations further. There is less need to include physical constants like μ_0 and k_B as they are implicit in the quantities.

Hence, we get normalized MHD equations of the form:

$$\frac{\partial \bar{n_s}}{\partial \bar{t}} + \nabla \cdot (\bar{n_s}\bar{\mathbf{v}_s}) = \bar{S} - \bar{L} \tag{3.18}$$

$$\begin{aligned} &\frac{\partial \bar{n}\bar{\mathbf{V}}}{\partial \bar{t}} + \nabla \cdot (\bar{\mathbf{K}} + \frac{\bar{B}^2}{2}\mathbf{I} - \bar{\mathbf{B}}\bar{\mathbf{B}}) \\ &= -(\bar{n}\bar{\nu}_{in} + \bar{m_e}\bar{n}\bar{\nu}_{en})(\bar{\mathbf{V}} + \bar{m_e}\bar{\mathbf{J}} - \bar{\mathbf{U}}) + \bar{m_e}(\bar{\nu}_{en} - \bar{\nu}_{in})\bar{\mathbf{J}} \\ &+ (\bar{S}\bar{m_n}\mathbf{U} - \bar{L}(\bar{\mathbf{V}} + \frac{\bar{m_e}}{1+\bar{m_e}}\bar{\mathbf{J}}) - \bar{L}\bar{m_e}(\bar{\mathbf{V}} - \bar{\mathbf{J}})) \end{aligned} \tag{3.19}$$

Chapter 4

Chromosphere Dynamics

4.1 Simulation Domain

Chapter 5

Conclusion

Bibliography

Eugene H. Avrett and Rudolf Loeser. Models of the solar chromosphere and transition region from sumer and hrts observations: Formation of the extreme-ultraviolet spectrum of hydrogen, carbon, and oxygen. *The Astrophysical Journal Supplement Series*, 175(1):229, 2008. URL http://stacks.iop.org/0067-0049/175/i=1/a=229.

D. N. Baker, X. Li, A. Pulkkinen, C. M. Ngwira, M. L. Mays, A. B. Galvin, and K. D. C. Simunac. A major solar eruptive event in july 2012: Defining extreme space weather scenarios. *Space Weather*, 11(10):585–591. doi: 10.1002/swe.20097. URL https://agupubs.onlinelibrary.wiley.com/doi/abs/10.1002/swe.20097.

W. Baumjohann and R.A. Treumann. *Basic Space Plasma Physics*. Imperial College Press, 1997. ISBN 9781860940798. URL https://books.google.com/books?id=bbVACbm9FjYC.

C. S. Brady and T. D. Arber. Simulations of alfvén and kink wave driving of the solar chromosphere: Efficient heating and spicule launching. *The Astrophysical Journal*, 829(2):80, 2016. URL http://stacks.iop.org/0004-637X/829/i=2/a=80.

B. de Pontieu, S. McIntosh, V. H. Hansteen, M. Carlsson, C. J. Schrijver, T. D. Tarbell, A. M. Title, R. A. Shine, Y. Suematsu, S. Tsuneta, Y. Katsukawa, K. Ichimoto, T. Shimizu, and S. Nagata. A Tale of Two Spicules: The Impact of Spicules on the Magnetic Chromosphere. , 59:S655–S662, November 2007. doi: 10.1093/pasj/59.sp3.S655.

A. Dedner, F. Kemm, D. Kröner, C.-D. Munz, T. Schnitzer, and M. Wesenberg.

Hyperbolic Divergence Cleaning for the MHD Equations. *Journal of Computational Physics*, 175:645–673, January 2002. doi: 10.1006/jcph.2001.6961.

C. C. Finlay, B. Langlais, F. J. Lowes, M. Mandea, M. Menvielle, L. Tøffner-Clausen, N. Olsen, A. Tangborn, Z. Wei, C. Manoj, S. Maus, S. McLean, A. W. P. Thomson, B. Hamilton, C. D. Beggan, S. Macmillan, T. A. Chernova, T. I. Zvereva, T. N. Bondar, V. P. Golovkov, A. Chambodut, A. Chulliat, E. Thébault, G. Hulot, H. Lühr, I. Michaelis, I. Wardinski, J. Rauberg, M. Hamoudi, M. Rother, V. Lesur, R. Holme, T. J. Sabaka, and W. Kuang. International Geomagnetic Reference Field: the eleventh generation. *Geophysical Journal International*, 183(3):1216–1230, 12 2010. ISSN 0956-540X. doi: 10.1111/j.1365-246X.2010.04804.x. URL `https://dx.doi.org/10.1111/j.1365-246X.2010.04804.x`.

A. H. Gabriel. A magnetic model of the solar transition region. *Philosophical Transactions of the Royal Society of London Series A*, 281:339–352, May 1976. doi: 10.1098/rsta.1976.0031.

Florian Rudolf Josef Weinbub Andreas Morhammer Tibor Grasser Ansgar Jüngel Karl Rupp, Philippe Tillet and Siegfried Selberherr. Viennacl - linear algebra library for multi- and many-core architectures, 2016. URL `http://viennacl.sourceforge.net/`.

Delores J. Knipp. Fall 2018 agu editors' highlights: Living within the sun's stormy atmosphere. *Space Weather*, 17(1):3–5. doi: 10.1029/2019SW002154. URL `https://agupubs.onlinelibrary.wiley.com/doi/abs/10.1029/2019SW002154`.

Delores J. Knipp, Brian J. Fraser, M. A. Shea, and D. F. Smart. On the little-known consequences of the 4 august 1972 ultra-fast coronal mass ejecta: Facts, commentary, and call to action. *Space Weather*, 16(11):1635–1643. doi: 10.1029/2018SW002024. URL `https://agupubs.onlinelibrary.wiley.com/doi/abs/10.1029/2018SW002024`.

Alexander Kurganov and Eitan Tadmor. New high-resolution central schemes for nonlinear conservation laws and convection–diffusion equations. *Journal of Compu-*

tational Physics, 160(1):241 – 282, 2000. ISSN 0021-9991. doi: https://doi.org/10.1006/jcph.2000.6459. URL http://www.sciencedirect.com/science/article/pii/S0021999100964593.

B. Kuźma, K. Murawski, T. V. Zaqarashvili, P. Konkol, and A. Mignone. Numerical simulations of solar spicules: Adiabatic and non-adiabatic studies. , 597:A133, January 2017. doi: 10.1051/0004-6361/201628747.

I. Langmuir. Oscillations in Ionized Gases. *Proceedings of the National Academy of Science*, 14:627–637, August 1928. doi: 10.1073/pnas.14.8.627.

Juan Martínez-Sykora, Bart De Pontieu, Mats Carlsson, Viggo H. Hansteen, Daniel Nóbrega-Siverio, and Boris V. Gudiksen. Two-dimensional radiative magnetohydrodynamic simulations of partial ionization in the chromosphere. ii. dynamics and energetics of the low solar atmosphere. *The Astrophysical Journal*, 847(1):36, 2017. URL http://stacks.iop.org/0004-637X/847/i=1/a=36.

S. W. McIntosh, B. de Pontieu, M. Carlsson, V. Hansteen, P. Boerner, and M. Goossens. Alfvénic waves with sufficient energy to power the quiet solar corona and fast solar wind. , 475:477–480, July 2011. doi: 10.1038/nature10235.

A. Mignone, P. Tzeferacos, and G. Bodo. High-order conservative finite difference GLM-MHD schemes for cell-centered MHD. *Journal of Computational Physics*, 229:5896–5920, August 2010. doi: 10.1016/j.jcp.2010.04.013.

P L Roe. Characteristic-based schemes for the euler equations. *Annual Review of Fluid Mechanics*, 18(1):337–365, 1986. doi: 10.1146/annurev.fl.18.010186.002005. URL https://doi.org/10.1146/annurev.fl.18.010186.002005.

R. J. Rutten. Observing the Solar Chromosphere. In P. Heinzel, I. Dorotovič, and R. J. Rutten, editors, *The Physics of Chromospheric Plasmas*, volume 368 of *Astronomical Society of the Pacific Conference Series*, page Heinzel, May 2007.

Conrad Sanderson and Ryan Curtin. Armadillo: a template-based c++ library for linear algebra, 2016. URL http://arma.sourceforge.net/.

P. Song and V. M. Vasyliūnas. EFFECT OF HORIZONTALLY INHOMOGENEOUS HEATING ON FLOW AND MAGNETIC FIELD IN THE CHROMOSPHERE OF THE SUN. *The Astrophysical Journal*, 796(2):L23, nov 2014. doi: 10.1088/2041-8205/796/2/l23. URL https://doi.org/10.1088%2F2041-8205%2F796%2F2%2Fl23.

Lewi Tonks. The birth of plasma. *American Journal of Physics*, 35(9):857–858, 1967. doi: 10.1119/1.1974266. URL https://doi.org/10.1119/1.1974266.

Jiannan Tu and Paul Song. A study of alfvén wave propagation and heating the chromosphere. *The Astrophysical Journal*, 777(1):53, 2013. URL http://stacks.iop.org/0004-637X/777/i=1/a=53.

V. M. Vasyliūnas and P. Song. Meaning of ionospheric Joule heating. *Journal of Geophysical Research (Space Physics)*, 110:A02301, February 2005. doi: 10.1029/2004JA010615.

Appendix A

Appendix Chapter